Molecular Crystals and Liquid Crystals
Publication details, including instructions for authors and subscription information:
http://www.tandfonline.com/loi/gmcl16

Solution and Solid State Studies of Tetrafluoro-7,7,8,8-Tetracyano-p-Quinodimethane, TCNQF4. Evidence for Long-Range Amphoteric Intermolecular Interactions and Low-Dimensionality in the Solid State Structure

Thomas J. Emge [a], Macrae Maxfield [a], Dwaine O. Cowan [a] & Thomas J. Kistenmacher [a]
[a] Department of Chemistry, The Johns Hopkins University, Baltimore, Maryland, 21218.
Version of record first published: 20 Apr 2011.

To cite this article: Thomas J. Emge , Macrae Maxfield , Dwaine O. Cowan & Thomas J. Kistenmacher (1981): Solution and Solid State Studies of Tetrafluoro-7,7,8,8-Tetracyano-p-Quinodimethane, TCNQF4. Evidence for Long-Range Amphoteric Intermolecular Interactions and Low-Dimensionality in the Solid State Structure, Molecular Crystals and Liquid Crystals, 65:3-4, 161-178

To link to this article: http://dx.doi.org/10.1080/00268948108082132

Mol. Cryst. Liq. Cryst., 1981, Vol. 65, pp. 161–178
0026-8941/81/6504–0161$06.50/0

Solution and Solid State Studies of Tetrafluoro-7,7,8,8-Tetracyano-*p*-Quinodimethane, TCNQF4. Evidence for Long-Range Amphoteric Intermolecular Interactions and Low-Dimensionality in the Solid State Structure

THOMAS J. EMGE, MacRAE MAXFIELD, DWAINE O. COWAN, and THOMAS J. KISTENMACHER

Department of Chemistry, The Johns Hopkins University, Baltimore, Maryland 21218.

(*Received July 7, 1980*)

Solution and solid state studies of TCNQF4 are reported. The electron affinity of TCNQF4 has been derived from spectral observations of the visible-near IR charge-transfer band for the pyrene complex and compared to that derived from the half-wave potentials used to characterize its reactivity in solution. It is demonstrated that the series, TCNQ, TCNQF to TCNQF4 shows a monotonic increase in reactivity with increasing fluorine substitution. Crystals of TCNQF4, grown from acetonitrile, are orthorhombic; space group Pbca, with the following crystal data: $a = 14.678(7)$A, $b = 9.337(5)$A, $c = 8.174(2)$A, $V = 1120.0(6)$A^3, $Z = 4$ [based on a molecular weight for $C_{12}N_4F_4 = 276.22$], $D_{measd} = 1.65(1)$ g cm^{-3}, $D_{calcd} = 1.64$ g cm^{-3}. Full matrix least-squares refinement (including anisotropic thermal parameters for all atoms) using 1763 counter-collected F_0's led to a final R value of 0.067 and a final weighted R value of 0.036. The observed molecular geometry of TCNQF4 is compared to that of its parent molecule TCNQ and to its monoanion found in some charge-transfer complexes. Crystal packing of TCNQF4 affords two interesting types of intermolecular acid/base (or donor/acceptor) interactions utilizing the cyano nitrogen atoms and the fluorinated carbon atoms of the quininoid ring. This subtle amphoterism exhibited by TCNQF4 leads to reduced dimensionality for the crystalline motif and is compared to similar solid state interactions found in several other molecules with π-bonded ring systems containing highly-electronegative substituents.

INTRODUCTION

The synthesis[1] of 2,3,5,6-tetrafluoro-7,7,8,8-tetracyano-*p*-quinodimethane, TCNQF4, like that of other halo- and alkyl-substituted derivatives[2] of the parent molecule TCNQ, has been completed in an effort to find new electron acceptor molecules for organic charge-transfer complexes. Donor-TCNQF4 complexes studied to date are mainly insulators, possibly having complete or nearly complete charge transfer.[3] A particularly interesting example is the segregated-stack complex HMTSF (hexamethylenetetraselenafulvalene)-TCNQF4, a Mott–Hubbard insulator,[4] which is isostructural with HMTSF–TCNQ, a quasi one-dimensional conductor.[5] The degree of charge transfer is of central importance to electron mobility and crystal cohesion in complexes containing segregated donor and acceptor chains. A theory of molecular Coulomb repulsion proposed by Bloch[6] appears to rationalize the degree of charge transfer in many donor-acceptor complexes and is entirely described by a set of chemical potentials analogous to electron affinities (EA's). The theory[6] predicts that combinations of donors and acceptors with large IP (donor)–EA (acceptor) differences (spanning hundreds of meV) will all have essentially unit charge transfer.

The electron affinity of TCNQF4 reported here and measured elsewhere,[7] in relation to other fluorinated TCNQ's and TCNQ itself, is so high that the critical IP–EA difference is small for virtually all donors examined to date.[3] In order to accurately discuss the relationship of charge transfer to electrical conductivity and crystal cohesion, it is essential to have evidence, in the solid state, for actual charge transfer for both conducting and insulating materials. Among the various schemes[8] that have been employed to measure the degree of charge transfer in donor-TCNQ complexes, one method[8–11] makes use of the coherent change in molecular geometry for the donor and acceptor components with charge transfer. Thus, we have undertaken a detailed analysis of the molecular geometry of neutral TCNQF4 by X-ray diffraction methods in order to provide a zero charge-transfer limit geometry.

In addition, there has been considerable speculation[12–13] about the relationship between the mode of intermolecular interaction observed in neutral donor and acceptor molecules and that observed in their charge-transfer salts. For example, the mode of intermolecular interaction for the donor TTF (tetrathiafulvalene) as a neutral solid[14] is very similar to that observed in its charge-transfer salt with TCNQ.[15] In contrast, the mode of intermolecular interaction in solid TCNQ[16] is quite different from that found in TTF–TCNQ.[15] In general, these interactions can be described as acid/base (or donor/acceptor) in character.[17–18] and range from ionic, as probably in alkali metal salts, to weakly covalent, as in HMTSF–TCNQ and HMTSF–TCNQF4, to dipolar, as exhibited by many π-bonded molecules with highly

electronegative substituents (e.g. chloranil).[19–21] Accordingly, the molecular packing motif and intermolecular interactions in solid TCNQF4 are of themselves important and, particularly, in comparison to that displayed by its charge-transfer complexes.

We wish then to report here on the determination of the molecular geometry and crystalline motif for TCNQF4, as well as the experimental determination of its electron affinity by solution spectroscopic and cyclic-voltammetric methods.

EXPERIMENTAL

Preparation

The TCNQF4 employed in this study was synthesized according to the procedure of Wheland and Martin.[1] Repeated recrystallization from dry acetonitrile, followed by gradient sublimation, gave crystals of adequate purity.

Solution and spectral studies

The visible-near IR charge-transfer spectra were obtained for pyrene complexes of TCNQF4 and other acceptors in methylene chloride. From the λ_{max} of these spectra, the energy of the charge-transfer band (E_{CT}) was obtained and used to derive the electron affinities of the various acceptor molecules. Independent measures of the electron affinities were obtained by cyclicvoltammetry from half-wave reduction potentials versus $Ag/AgNO_3$ and saturated calomel electrodes in 0.1 M tetrabutyl-ammonium tetrafluoroborate in butylonitrile at 22°C.

Diffraction studies

Large, single crystals of TCNQF4 were obtained after complete evaporation of the acetonitrile solvent at room temperature. The data crystal employed in our study had well-developed natural faces and was free from observable imperfections. Subsequent grinding of this crystal gave a symmetrically-shaped ellipsoid 0.402 mm long by 0.350 mm in radial cross-section. Mounting along the principal axis resulted in an orientation approximately about the crystallographic c axis.

The crystal density was measured by the neutral buoyancy method in a mixture of carbon tetrachloride and bromoform. Preliminary photographic recording of the intensity-weighted reciprocal lattice indicated that the

crystal system was orthorhombic, and the observed systematic absences ($0kl$, $k = 2n + 1$; $h0l$, $l = 2n + 1$; $hk0$, $h = 2n + 1$) were consistent with the space group Pbca. The measured density allowed the presence of four molecules per cell, requiring that the TCNQF4 molecule display at least $\bar{1}(C_i)$ molecular symmetry.

Unit-cell dimensions and their associated standard deviations were obtained from a least-square fit to the setting angles of 15 carefully-centered reflections measured on a Syntex $P\bar{1}$ automated diffractometer. Standard crystallographic data are as follows: $a = 14.678(7)$A, $b = 9.337(5)$A, $c = 8.174(2)$A, V = 1120.0(6)A^3, Z = 4, $D_{measd} = 1.65(1)$ g cm^{-3}, $D_{calcd} = 1.64$ g cm^{-3}. The 7237 reflections in the +h-hemisphere to $2\theta = 62°$ were surveyed on the diffractometer, employing graphite-monochromatized MoK$\bar{\alpha}$ radiation and the $\theta/2\theta$ scan mode. A constant scan rate of 1.5 degrees (2θ) per minute was maintained for each diffraction peak. Three standards were monitored after every 100 reflections, and their intensities showed no unusual variation throughout the course of the experiment. A symmetry-averaged set of 1763 non-zero reflections was used as the basis of the structural solution and refinement. The R value on averaging over the four octants of data was 0.016 [$R_{ave} = \sum_{i=1}^{N} \sum_{j=1}^{n} |F_{ij}^2 - \bar{F}_i^2| / \sum_{i=1}^{N} \bar{F}_i^2$, where N = the total number of unique observations and n = the number of independent times each observation was measured]. An approximate scale factor was derived by the method of Wilson.[22]

Positional parameters for all atoms were obtained by a combination of unsharpened and sharpened ($E^2 - 1$) Patterson methods followed by Fourier and difference-Fourier syntheses. Full-matrix least-squares refinement (all atoms treated anisotropically and minimizing the quantity $\sum w(|F_o| - |F_c|)^2$ where $w = 4F_o^2/\sigma^2(F_o^2)$ led to a final R value [$\sum ||F_o| - |F_c|| / \sum |F_o|$] of 0.067 and a final weighted R value [$\{\sum w(|F_o| - |F_c|)^2 / \sum w|F_o|^2\}^{1/2}$] of 0.036. The derived value for the goodness of fit [$\{\sum w(|F_o| - |F_c|)^2/(NO-NV)\}^{1/2}$, where NO = 1763 observations and NV = 91 variables] was 2.56. A final difference-Fourier map was essentially featureless (residual density peaks lying between ± 0.25 e/A^3), restricting attempts to resolve deformation density information.

Neutral scattering factors for all atoms were taken from the compilation of Hanson, Herman, Lea and Skillman.[23] The scattering curves were corrected for anomalous dispersion effects.[24] Final atomic positional and thermal parameters (U_{ij}'s) are given in Table I, where we also include the differences in U_{ij} between the final least-squares values and those calculated from a rigid-body treatment of the tetrafluoroquininoid framework utilizing the method of Schomaker and Trueblood.[25] The RMS difference between least-squares and the rigid-body U_{ij}'s is 0.0017A^2, indicating that the tetrafluoroquininoid framework can be effectively treated as a rigid body.[25] We

have employed the librational tensor obtained from the rigid-body analysis to obtain corrected positional coordinates and derived bond lengths and angles (*vide infra*).[26]

TABLE I

Final atomic parameters for TCNQF4

Estimated standard deviations are enclosed in parentheses. The fractional coordinates and anisotropic thermal parameters[a] have been multiplied by 10^4

Atom	*x*	*y*	*z*
C(1)	809(1)	740(1)	27(1)
C(2)	−292(1)	−797(1)	1313(1)
C(3)	570(1)	−81(1)	1452(1)
C(4)	1120(1)	−176(1)	2805(2)
C(5)	1982(1)	536(2)	2962(2)
C(6)	884(1)	−982(1)	4245(2)
N(1)	2663(1)	1077(1)	3212(2)
N(2)	729(1)	−1565(1)	5441(1)
F(1)	1582(1)	1492(1)	68(1)
F(2)	−580(1)	−1585(1)	2578(1)

Atom	U_{11}	U_{22}	U_{33}	U_{12}	U_{13}	U_{23}
C(1)	478(6)	461(6)	636(7)	−69(5)	112(6)	−39(6)
	[−5][b]	[0]	[−9]	[−36]	[−5]	[−28]
C(2)	563(7)	436(6)	567(6)	−54(6)	146(6)	18(6)
	[56]	[−2]	[−59]	[−35]	[21]	[19]
C(3)	503(6)	406(6)	575(7)	19(5)	119(6)	−48(5)
	[34]	[22]	[−39]	[−17]	[0]	[−6]
C(4)	530(7)	484(7)	628(8)	46(6)	87(6)	−20(6)
	[−6]	(4)	[−20]	[−1]	[15]	[23]
C(5)	560(8)	701(9)	722(9)	27(7)	7(7)	22(7)
	[−8]	[−28]	[−38]	[65]	[4]	[57]
C(6)	611(8)	561(8)	690(9)	38(6)	−3(7)	−3(7)
	[-98]	[−20]	[35]	[5]	[−40]	[−22]
N(1)	651(8)	1123(12)	1059(10)	−111(8)	−74(7)	32(9)
	[0]	[42]	[146]	[78]	[12]	[25]
N(2)	880(8)	794(8)	747(7)	−60(7)	−41(7)	127(7)
	[−55]	[6]	[58]	[−2]	[−34]	[7]
F(1)	629(4)	749(5)	763(5)	−257(4)	70(4)	13(4)
	[28]	[−25]	[−11]	[−33]	[11]	[−65]
F(2)	741(5)	691(4)	631(4)	−174(4)	107(4)	108(4)
	[54]	[0]	[−64]	[−6]	[15]	[−9]

[a] The anisotropic thermal ellipsoid is defined by the equation:

$$\exp[-2\Pi^2\{U_{11}(a*h)^2 + U_{22}(b*k)^2 + U_{33}(c*l)^2 + 2U_{12}(a*b*hk) + 2U_{13}(a*c*hl) + 2U_{23}(b*c*kl)\}].$$

[b] Differences in U_{ij} between final least-square refinement values and libration-corrected values are included in square brackets.

The crystallographic computations were carried out with a standard set of computer programs.[27] Illustrations were prepared with the aid of ORTEP.[28]

RESULTS AND DISCUSSION

(a) Molecular geometry of the TCNQF4 molecule

Both uncorrected and libration-corrected intramolecular bond lengths and angles for TCNQF4, illustrated in Figure 1, are collected in Table II. The correction to the molecular geometry for librational effects are small (on the order of 0.001A to 0.006A), although—as in the analysis of TCNQ[16]—the computed corrections to the terminal cyano group bond lengths are probably underestimated by about a factor of 2. A comparison of the molecular geometry of TCNQF4 and TCNQ completes Table II.

A detailed analysis of the bond lengths in TCNQF4 and TCNQ from Table II reveals only two minor differences. The formal ring double bond, C(1)—C(2′), and one of the adjacent formal single bonds, C(2)—C(3), are about 0.01A shorter than in TCNQ. These differences are quite possibly related to the presence of the fluoro substituents in TCNQF4, but obviously

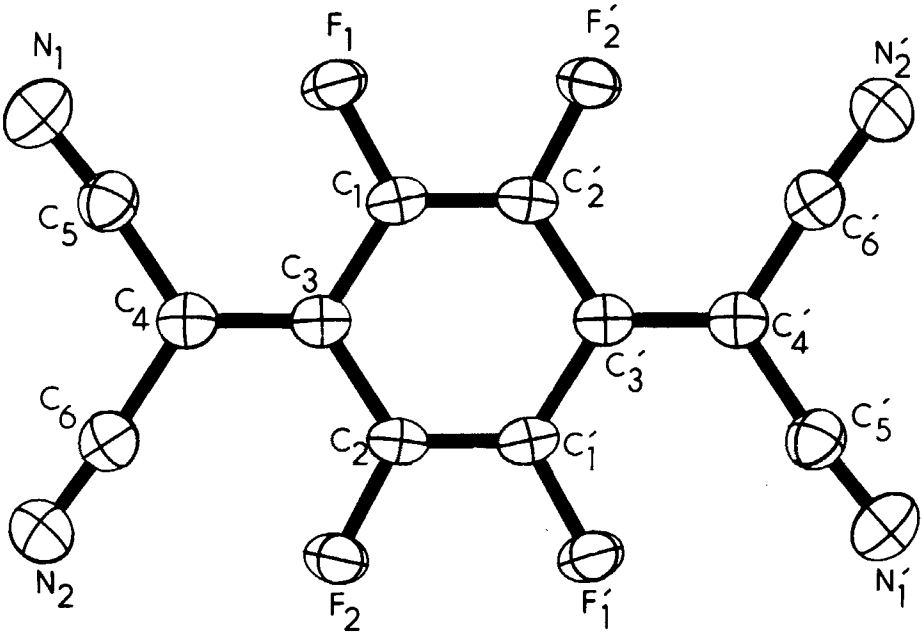

FIGURE 1 An illustration of a single TCNQF4 molecule. The thermal ellipsoids are drawn at the 30% probability level.

TABLE II

Comparison of the bond lengths and angles in TCNQF4 and TCNQ

(a) Bond lengths

Bond	*TCNQF4*	*TCNQ*
C(1)—C(2*)[a]	1.334(2) [1.336]	1.344(3) [1.346]
C(1)—C(3)	1.438(2) [1.443]	1.440(4) [1.446]
C(2)—C(3)	1.436(2) [1.442]	1.445(4) [1.450]
C(3)—C(4)	1.372(2) [1.374]	1.373(3) [1.374]
C(4)—C(5)	1.435(2) [1.441]	1.436(4) [1.441]
C(4)—C(6)	1.439(2) [1.445]	1.435(4) [1.440]
N(1)—C(5)	1.139(2) [1.141]	1.139(3) [1.141]
N(2)—C(6)	1.142(2) [1.145]	1.137(3) [1.139]
F(1)—C(1)	1.335(1) [1.336]	
F(2)—C(2)	1.338(1) [1.341]	

(b) Bond angles

Angle	*TCNQF4*	*TCNQ*
C(3)—C(1)—C(2*)	123.2(1) [123.0]	121.1(2) [121.0]
C(3)—C(2)—C(1*)	123.2(1) [123.2]	120.8(2) [120.7]
C(1)—C(3)—C(2)	113.5(1) [113.7]	118.1(2) [118.3]
C(1)—C(3)—C(4)	123.0(1) [122.8]	121.1(2) [121.0]
C(2)—C(3)—C(4)	123.5(1) [123.5]	120.8(2) [120.7]
C(3)—C(4)—C(5)	124.1(1) [124.1]	122.1(2) [122.0]
C(3)—C(4)—C(6)	123.5(1) [123.3]	121.9(2) [121.8]
C(5)—C(4)—C(6)	112.4(1) [112.6]	115.9(2) [116.1]
N(1)—C(5)—C(4)	174.7(1) [174.7]	179.4(2) [179.4]
N(2)—C(6)—C(4)	175.8(1) [175.8]	179.6(2) [179.6]
F(1)—C(1)—C(3)	117.9(1) [118.0]	

TABLE II (*continued*)

Comparison of the bond lengths and angles in TCNQF4 and TCNQ

(b) Bond angles

Angle	*TCNQF4*	*TCNQ*
F(1)—C(1)—C(2*)	118.9(1) [118.9]	
F(2)—C(2)—C(3)	118.3(1) [118.4]	
F(2)—C(2)—C(1*)	118.5(1) [118.4]	

[a] An asterisk signifies the following transformation: $\bar{x}$, $\bar{y}$, $\bar{z}$.

[b] Standard deviations of the least-significant digit are given in parentheses.

[c] Libration-corrected values are given in square brackets.

it is in the intramolecular bond angles that the effects of the fluoro substituents are predominantly displayed. The endocylic ring angles about the carbon atoms C(1) and C(2) and the exocyclic bond angles about atom C(3) have all expanded by $\sim 2°$ on going from TCNQ on TCNQF4. In contrast, the endocyclic bond angle about atom C(3) has contracted by $\sim 5°$. These bond angle changes are in the same direction but considerably larger in magnitude than Rees[29] has observed in the series *p*-benzequinone, chloro-*p*-benzoquinone, dichloro-*p*-benzoquinone through tetrachloro-*p*-benzoquinone(chloranil). We attribute the increased influence of the fluoro over the chloro substituents to the considerably shorter C—F versus the C—Cl bond length (1.34A and 1.71A, respectively) and the concomitant increase in the intramolecular steric repulsion. Consistent with this interpretation are the increase in the C(3)—C(4)—C(5) and C(3)—C(4)—C(6) bond angles by $\sim 2°$ and the concurrent decrease in the C(5)—C(4)—C(6) bond angle by 3.5°, each of these effects being attributed to intramolecular repulsion between the malonitrile moiety and the fluoro substituents. Thus, TCNQF4 can be added to the ranks of "crowded" organic molecules.

The average C—F bond length in TCNQF4 of 1.336(1)A agrees well with the typical value of 1.35A determined by Yokozeki and Bauer[30] from a variety of compounds containing $C(sp^2)$-F bonds. In particular, the observed C—F distance in TCNQF4 lies, as expected, between those found for mono- and di-fluorobenzene (1.35 and 1.31A, respectively).[31-32]

The TCNQF4 molecule is moderately planar, displaying nearly mmm(D_{2h}) molecular symmetry although only $\bar{1}(C_i)$ symmetry is crystallographically

required. In Table III we present a least-square analysis of the benzenoid ring of the TCNQF4 and note the deviations of all atoms from this plane. Qualitatively, the deviations from planarity of the TCNQF4 molecule are five to ten times larger than for the TCNQ molecule.[16] The increased non-planarity in TCNQF4 is again probably a direct result of minimizing intramolecular repulsive interactions in this "crowded" molecule.

TABLE III

Planarity of the benzenoid ring in TCNQF4 and deviations (A) of individual atoms from this plane

In the equation of the plane below, X, Y, and Z are coordinates (A) referred to the orthogonal axes X along a, Y along b, and Z along c. Atoms indicated by an asterisk were given zero weight in calculating the plane; all other atoms were equally weighted

$(0.4671X - 0.8007Y - 0.3751Z = 0.0000\text{A})$

C(1)	∓ 0.007	C(4)*	± 0.040
C(2)	∓ 0.007	C(5)*	± 0.050
C(3)	± 0.006	C(6)*	± 0.039
N(1)*	± 0.036	F(1)*	∓ 0.052
N(2)*	± 0.002	F(2)*	∓ 0.003

Finally, the observed geometry of neutral TCNQF4 can be compared to that of its anion in some charge-transfer complexes. We have examined in detail the structures of HMTSF–TCNQF4[33] and DBTTF(dibenzotetrathiafulvalene)–TCNQF4.[34] In comparing the TCNQF4 bond lengths in these charge-transfer complexes to those in TCNQF4 reported here, we find (in accord with theoretical considerations and experimental observations of TCNQ systems)[8] that the most effected bond length is the exocyclic C=C bond of the quininoid ring. The charge-transfer complexes exhibit values for this bond [1.405(5)A for the HMTSF complex[33] and 1.412(6)A for the DBTTF complex][34] which are about 0.04A longer than in neutral TCNQF4 [1.372(2)A]. As in the TCNQ complexes, this elongation arises probably from the population of the frontier LUMO which is antibonding in character for the C(3)—C(4) double bond.[35] If a similar bond length change versus charge transfer correlation exists for TCNQF4 complexes as for TCNQ complexes,[8] then the bond length elongations in HMTSF–TCNQF4 and DBTTF–TCNQF4 are suggestive of nearly unit charge transfer. This

deduction from molecular geometry considerations is in excellent agreement with the degree of charge transfer obtained from other physical properties of these TCNQF4 complexes.[6,36]

(b) Intermolecular interactions and crystal packing

The crystal structure of TCNQF4 displays two interesting short contacts between symmetry-related molecules. One of these contacts, N(1) --- C(1)[$\frac{1}{2} - x, -y, \frac{1}{2} + z$] is observed at 3.18A and lies just short of the expected sum of the van der Walls radii (3.20–3.25A), Figure 2B. The other of these contacts, N(2) --- C(2), is found at 2.97A—less than the sum of the van der Walls radii by 0.23–0.28A, Figure 2A. Each TCNQF4 molecule in the solid partakes in a total of eight such acid/base interactions, four of which are shown for the central molecule in the unit-cell stereoview of the crystal structure presented in Figure 3.

The weaker N(1) --- C(1) interaction is identical in magnitude to the 3.18A N --- C contact observed in the structure of TCNQ.[16] However, for TCNQ, the crystal packing is dominated by the parallel stacking of two molecules in a ring-over-cyano group motif,[16] Figure 2C. This stacking mode in TCNQ somewhat resembles the ring-over-quininoid double bond mode observed in many donor-acceptor complexes containing charged TCNQ anions.[37] In the herringbone arrangement found in the structure of TCNQ,[16] the dihedral angle between interacting dimers is 48.0°. This small dihedral angle is comparable to that (44.1°) between planes which show the similarly weak N(1) --- C(1) contact in the structure of TCNQF4.

Certainly the most interesting feature of the structure of TCNQF4 is the strong N(2) --- C(2) interaction. Primarily on the basis of this contact, one may characterize the TCNQF4 molecule as being amphoteric—that is, it acts as both a base (donor) through its electron-rich cyano groups, and an acid (acceptor) through its electron-deficient fluorinated ring carbon atoms.

Similar acid/base amphoterism has been studied extensively, including the carbonyl-oxygen-atom-to-carbonyl-carbon-atom interaction in parabamic acid,[38] barbituric acid[39] and chloranil.[19] Particularly, the intermolecular interactions in the structure of chloranil[19] provide an excellent analogy for the acid/base interactions found in the structure of TCNQF4. There is a weak intermolecular contact at 3.06A between the electron-rich carbonyl oxygen atom and a chlorinated, electron-deficient, benzenoid carbon atom of a symmetry-related chloranil molecule. The strongest intermolecular contact in chloranil, however, is that of 2.85A, which occurs between the carbonyl oxygen atom of one molecule and the carbonyl carbon atom of another molecule. Figure 2D. The two contacts in chloranil are rather short in comparison to the expected sum of the van der Waals radii (by

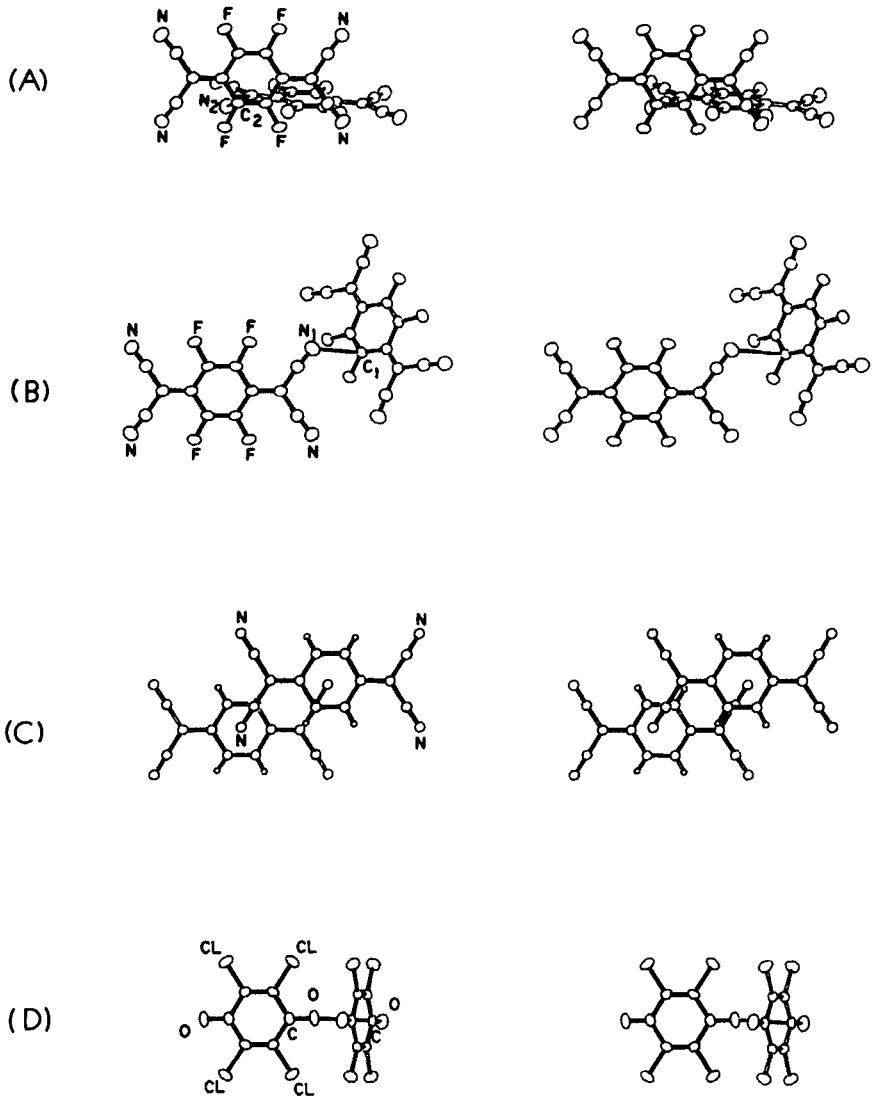

FIGURE 2 Comparison of intermolecular interaction geometries for selected molecules. The view direction is normal to the least-squares molecular plane of the shaded molecule in each case. (A) TCNQF4, N(2) --- C(2; x, $\frac{1}{2} - y$, $\frac{1}{2} + z$) interaction (3.18A). (B) TCNQF4, N(1) --- C(1; $\frac{1}{2} - x$, $\bar{y}$, $\frac{1}{2} + z$) interaction (2.97A). Projection view on the parallel overlap of two TCNQ molecules. (D) Chloranil, O(1) --- C(3; $\frac{1}{2} - x$, $\frac{1}{2} + y$, $\bar{z}$) interaction (2.85A).

about 0.04–0.09A for the weaker contact and by about 0.25–0.30A for the stronger contact—essentially the same ranges observed for the two contacts of interest in the structure of TCNQF4).

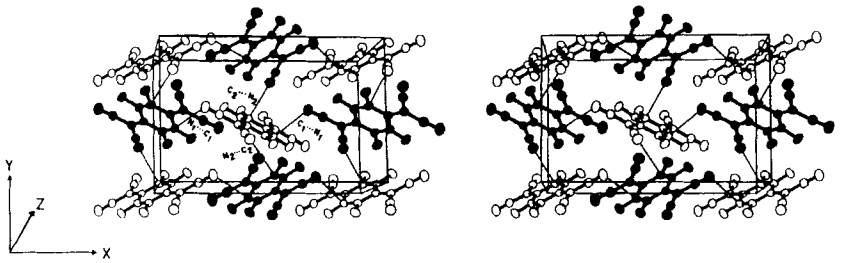

FIGURE 3 A stereoview (along c) of the packing in the unit cell for the TCNQF4 structure. All pertinent N ··· C interactions are shown for the central molecule.

An additional analysis of the strength of the interactions of TCNQF4 may be made on the basis of specific dihedral angles between interacting planes and the angles about atoms involved in the contacts.[20-21] In Table IV, we compare several features of the O ··· C intermolecular contacts for parabamic acid,[38] chloranil (from both room temperature and 110K X-ray diffraction data),[19] and barbituric acid[39] as well as the N ··· C contacts in TCNQF4 and TCNQ.[16] An interesting trend, besides the consistent decrease in the contact distance with increasing strength, is the opening of the dihedral angle between molecular planes to perhaps 90°. The dihedral angle between planes seems to be consistent in its sensitivity to the apparent strength of the interaction, even though this angle is affected by all aspects of the crystal packing. Similar observations have been made by Bürgi and

TABLE IV

Approaches and angles of selected compounds with interesting acid/base interactions

Compound		O ··· C	O ··· C=O	Dihedral
		distance (*A*)	*angle* (*deg*)	*angle* (*deg*)
Parabanic acid		2.77	90.8	70.9
Chloranil (110K)		2.77	99.5	68.3
Chloranil (298K)		2.85	99.4	67.7
Barbituric acid		2.90	106.2	67.1
TCNQF4		N ··· C	N ··· C—F	
		distance (*A*)	*angle* (*deg*)	
N(2)	C(2)	2.97	83.6	73.6
N(1)	C(1)	3.18	72.1	44.1
TCNQ			N ··· C=C	
			angle (*deg*)	
N(1)	C(4)	3.18	106.0	48.0

co-workers[18,21] in more elaborate tabulations. Also, the angles between the carbonyl oxygen atom and the contacted carbonyl group (similarly between the cyano nitrogen atom and the C—F group in TCNQF4) seem to indicate a preference for an interaction approach near right angles, advancing from the obtuse side for the O ··· C≡O contacts and from the acute side for the N ··· C—F contacts. These angles may be better indicators of dipolar strength than the C≡O ··· C angle or its counterpart in TCNQF4 the C≡N ··· C angle, which is inconsistent with the apparent trends observed for the carbonyl-containing compounds.

Finally, we wish to emphasize the fact that the strong N(2) ··· C(2) interaction observed in TCNQF4 allows, qualitatively, a reduction in the dimensionality of the crystal structure. In Figure 4, we present a projection of the TCNQF4 structure onto the *ac* crystallographic plane. It is clearly evident that the strong N(2) ··· C(2) contacts lie within planes parallel to the *bc* plane. The weaker N(1) ··· C(1) contacts serve to couple these planes of strongly interacting molecules. Thus, the structure of TCNQF4 can be considered as composed of strongly-coupled, two-dimensional layers

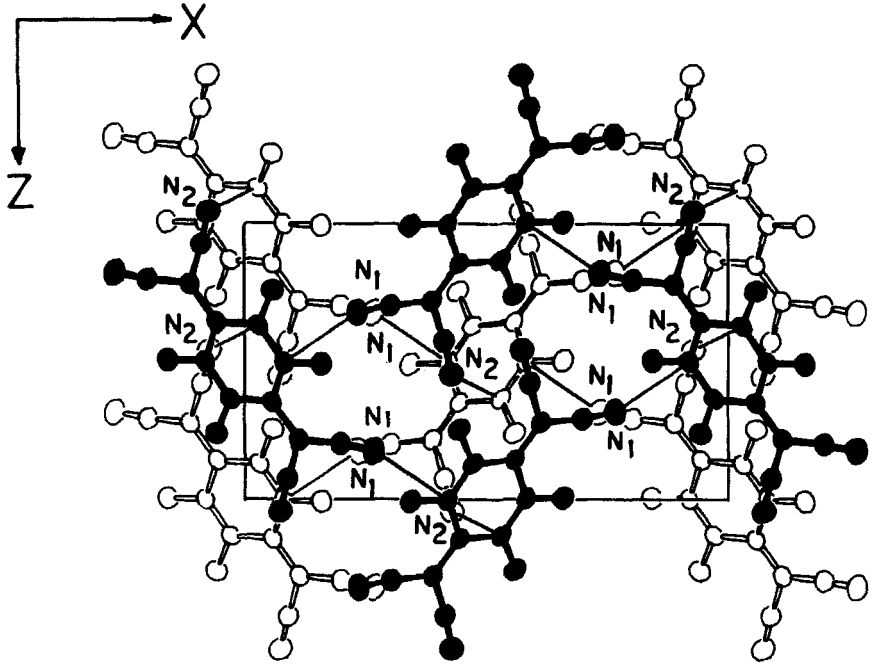

FIGURE 4 A projection of the structure of TCNQF4 onto the *ac* crystallographic plane. Note the presence of only interactions of the type N(2) ··· C(2) in the *bc* plane and the coupling of these planes through the weaker N(1) ··· C(1) interaction.

weakly extended to three dimensions. Similar dimensionality effects are a common characteristic of many charge-transfer complexes containing TCNQ and TCNQF4.[2,8,37]

(c) Cyclicvoltammetry results

The reactivity of acceptor and donor molecules is typically characterized by solution half-wave potentials whose values depend on reference electrode, electrolyte, solvent, and specific conditions of the cyclicvoltammetry. Although half-wave potentials for reversible one-electron transfers are convenient representations of electron affinity (EA), their reported values vary a great deal. In addition, the determination of absolute EA by thermal electron attachment[40] or magnetron[41] techniques is not available to most researchers.

We have adopted Eq. (1) from Chen and Wentworth[7] for obtaining

$$EA(CT) = IP + C - E_{CT} \tag{1}$$

acceptor EA's spectrophotometrically. Following the procedure of Merrifield and Phillips,[42] charge-transfer bands in the absorption spectrum were recorded for methylene chloride solutions of pyrene complexes with TCNQ, TCNQF, and TCNQF4. Electron affinities calculated from Eq. (1) [where $IP + C = 4.51 \pm 0.26$ eV] are plotted in Figure 5 versus first half-wave potentials recorded under identical conditions. The resulting linear relationships with unit slope follow Eq. (2),

$$EA(E_{1/2}) = E_{1/2}^{\text{red}} - \Delta G_{\text{sol}} - C, \tag{2}$$

where $\Delta G_{\text{sol}} = 2.53$ eV for butylronitrile and $C = -5.07$ eV for the saturated calomel and -5.45 eV for the $Ag/AgNO_3$ electrode.[43] The EA's calculated from Eqs. (1) and (2) are listed in Table V. A monotonic variation in EA with the number of fluoro substituents is observed. This linear relationship for $EA(CT)$ and $EA(E_{1/2})$ gives confidence to the $EA(CT)$ derived from Eq. (1). Similarly, the close agreement between the two sets of derived EA's suggests that reliable EA's for TCNQ-like molecules can be obtained from cyclicvoltammetry, once the constants in Eq. (2) are established for a specific set of conditions. We recommend that future studies characterize acceptors by EA's as well as by half-wave potentials.

Conclusions

The rather symmetrical molecular structure of TCNQF4 presents no unusual differences from that of its unfluorinated parent TCNQ, outside of the angular deformations induced by the steric demands of the fluoro substituents.

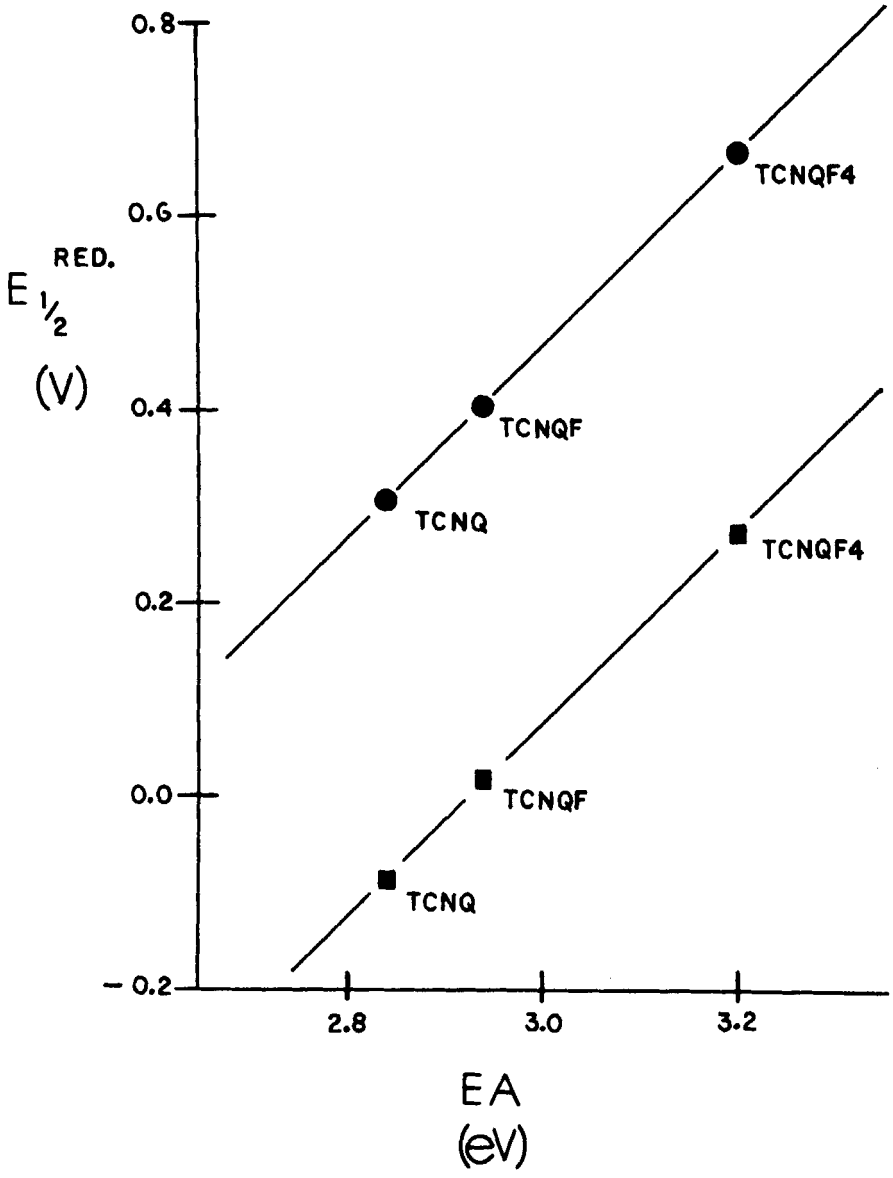

FIGURE 5 Plot of half-wave reduction potential versus electron affinity for TCNQ and some of its fluoro derivatives. Values indicated by ● are versus the standard calomel electrode, while those indicated by ■ are versus the $Ag/AgNO_3$ electrode.

TABLE V

Electron affinities derived from charge transfer energies and half-wave reduction potentials for pyrene complexes of TCNQ and some of its fluoro derivatives

Acceptor	$E^{red}_{1/2}$ vs SSCE[a] (volts)	$E^{red}_{1/2}$ vs $Ag/NgNO_3$[a] (volts)	$EA(E_{1/2})$[b] (eV)	$EA(CT)$[c] (eV)	E_{CT} (eV)
TCNQ	+0.30	−0.09	2.84	2.84	1.67
TCNQF	+0.40	+0.02	2.95	2.94 (2.95)[44]	1.57
TCNQF2				(3.02)[45]	
TCNQF4	+0.66	+0.27	3.20	3.20	1.31

[a] The reported half-wave potential is the mean value of the anodic current peak potential and its corresponding cathodic current peak potential recorded for dilute solution of the acceptor in butylronitile with 0.1 M tetrabutyl-ammonium tetrafluoroborate at 22°C.

[b] The calculated $EA(E_{1/2})$, with esd of ±0.01 eV, are based on the $E^{red}_{1/2}$ obtained from $Ag/AgNO_3$ electrode using Eq. (2) of the text.

[c] The calculated $EA(CT)$, with esd of ±0.01 eV, are based on the charge-transfer band energy, $E_{CT} = h/\lambda_{max}$, using Eq. (1) of the text.

Contrary to a ring-over-bond stacking mode displayed in the structure of TCNQ and in many donor-acceptor complexes of TCNQ and TCNQF4, the crystal structure of TCNQF4 is dominated by dipolar (acid/base) interactions. The short N ··· C—F contact of 2.97A and the dihedral angle between interacting molecules at 73.6° are both indicative of strong intermolecular association. Similar molecular associations have been reported for a variety of π-ring system molecules containing electronegative substituents, notably for carbonyl-containing species. For TCNQF4, the four strong acid/base contacts per molecule serve to produce a strongly-coupled, two-dimensional net, with extension to three-dimensions *via* four weaker acid/base contacts. The major difference between the TCNQF4 interactions and those observed in other systems is that the approach between interacting molecules does not take place along the direction of the polar axis of the π-bonded molecular orbital, as it does, for example, in chloranil. Otherwise, the crystal structure of chloranil provides an excellent comparison for both the weak and strong intermolecular interactions observed in the structure of TCNQF4. The strength of these interactions in each case is nearly identical, as judged by comparison of the distance of the interactions to their expected value based on sums of van der Waals radii. Particular trends of interaction strength are demonstrated for these intermolecular interactions, especially the interaction distance itself and the dihedral angle between molecular planes.

Lastly, the series TCNQ, TCNQF, and TCNQF4 shows a monotonic increase in electron affinity with the number of fluoro substituents based on spectroscopic and cyclicvoltammetric measurements. A knowledge of the

electron affinity variation in this series may provide critical information as to the choice of donor and acceptor components for organic charge-transfer complexes.

Acknowledgments

This investigation was supported by the National Science Foundation under grants DMR 76-84238 and DMR 78-23957. We particularly thank Mr Wayne A. Bryden for producing crystals of excellent quality and many helpful discussions. Also, we thank Prof. J. P. Ferraris for a sample of TCNQF.

Supplementary material

A list of calculated and observed structure factor amplitudes has been deposited.

References and footnotes

1. R. C. Wheland and E. L. Martin, *J. Org. Chem.*, **40**, 3101 (1975).
2. J. S. Miller and A. J. Epstein, eds., *Annals of the New York Academy of Sciences*, **313** (1978).
3. (a) W. A. Bryden, D. Deyo, A. N. Bloch, and D. O. Cowan, unpublished results; (b) W. A. Bryden, A. N. Bloch, and D. O. Cowan, unpublished results; (c) P. Shu and D. O. Cowan, unpublished results.
4. M. E. Hawley, T. O. Poehler, T. F. Carruthers, A. N. Bloch, D. O. Cowan, and T. J. Kistenmacher, *Bull. Am. Phys. Soc.*, **23**, 424 (1978).
5. T. E. Phillips, T. J. Kistenmacher, A. N. Bloch, and D. O. Cowan, *J. Chem. Soc., Chem. Commun.*, 334 (1976)
6. A. N. Bloch, *Bull. Am. Phys. Soc.*, **25**, 255 (1980).
7. E. C. M. Chen and W. E. Wentworth, *J. Chem. Phys.*, **63**, 3183 (1975).
8. T. J. Kistenmacher, A.I.P. Conf. Proc., No. 53, 193 (1979).
9. V. van Bodegom, J. L. de Boer, and A. Vos, *Acta Cryst.*, **B33**, 602 (1977).
10. P. Coppens and T. N. G. Row, *Annals of the New York Academy of Sciences*, **313**, 244 (1978).
11. P. S. Flandrois and D. Chasseau, *Acta Cryst.*, **B33**, 2744 (1977).
12. A. J. Berlinsky, *Contemp. Phys.*, **17**, 331 (1976).
13. B. D. Silverman, *J. Chem. Phys.*, **71**, 3592 (1979).
14. W. F. Cooper, N. C. Kenny, J. W. Edmonds, A. Nagel, F. Wudl, and P. Coppens, *Chem. Commun.*, 889 (1971).
15. T. J. Kistenmacher, T. E. Phillips, and D. O. Cowan, *Acta Cryst.*, **B30**, 763 (1974).
16. R. E. Long, R. A. Sparks, and K. N. Trueblood, *Acta Cryst.*, **18**, 932 (1965).
17. H. Bent, *Chem. Rev.*, **68**, 587 (1968).
18. H. B. Bürgi, *Angew. Chem. Internat. Edit.*, **14**, 460 (1975).
19. (a) S. S. C. Chu, G. A. Jeffrey, and T. Sakurai, *Acta Cryst.*, **15**, 661 (1962); (b) K. J. van Weperen and G. J. Visser, *Acta Cryst.*, **B28**, 338 (1972).
20. W. Bolton, *Nature*, **201**, 987 (1964).
21. H. B. Bürgi, J. D. Dunitz, and E. Shefter, *Acta Cryst.*, **B30**, 1517 (1974).
22. A. J. C. Wilson, *Nature* (London), **150**, 151 (1942).
23. H. P. Hanson, F. Herman, J. D. Lea, and S. Skillman, *Acta Cryst.*, **17**, 1040 (1964).
24. D. T. Cromer and D. Liberman, *J. Chem. Phys.*, **53**, 1891 (1970).
25. V. Schomaker and K. N. Trueblood, *Acta Cryst.*, **B24**, 63 (1968).
26. D. W. J. Cruikshank, *Acta Cryst.*, **9**, 757 (1956).
27. Crystallographic programs employed include: Wehe, Busing and Levy's ORABS: Busing, Martin, and Levy's ORFLS; Zalkins FORDAP; Pippy and Ahmed's MEAN PLANE.
28. Drawings made with use of Johnson's ORTEP.

29. (a) P. B. Rees, *Acta Cryst.*, **B26**, 1292 (1969); (b) P. B. Rees, *Acta Cryst.*, **B26**, 1298 (1969); (c) P. B. Rees, *Acta Cryst.*, **A26**, 1304 (1969); (d) P. B. Rees, *Acta Cryst.*, **B26**, 1311 (1969).
30. A Yokozeki and S. H. Bauer, *Top. Curr. Chem.*, **53**, 71 (1975).
31. L. Nygaard, I. Bojesen, T. Pedersen, and J. Rastrup-Anderson, *J. Mol. Structure*, **2**, 209 (1968).
32. L. Nygaard, R. L. Hansen, J. Rastrup-Anderson, and G. O. Sorensen, *Spectrochim. Acta*, **23B**, 2813 (1967).
33. T. J. Kistenmacher and T. J. Emge, to be published.
34. T. J. Emge and T. J. Kistenmacher, to be published.
35. (a) H. Johanson, *Int. J. Quant. Chem.*, **9**, 459 (1975); (b) R. C. Haddon, *Aust. J. Chem.*, **28**, 2333 (1975); (c) W. D. Grobman and B. D. Silverman, *Solid State Commun.*, **19**, 319 (1976).
36. J. S. Chappell, M. Maxfield, D. O. Cowan, and A. N. Block, unpublished results.
37. T. J. Kistenmacher, *Annals of the New York Academy of Sciences*, **313**, 333 (1978).
38. B. M. Graven, and R. K. McMullan, *Acta Cryst.*, **A35**, 934 (1979).
39. W. Bolton, *Acta Cryst.*, **16**, 166 (1963).
40. W. E. Wentworth, J. E. Lovelock, and E. C. Chen, *J. Chem. Phys.*, **70**, 445 (1966).
41. A. L. Farragher and T. M. Page, *Trans. Faraday Soc.*, **63**, 2369 (1967).
42. R. E. Merrifield and W. D. Phillips, *J. Am. Chem. Soc.*, **80**, 2778 (1958).
43. $\Delta G_{sol} - C$ was determined from the intercepts of the lines; the Chen and Wentworth[7] value of C for the SSCE electrode was used to extract ΔG_{sol} in butylronitrile, and from this calculated ΔG_{sol}, the constant for the $Ag/AgNO_3$ electrode was estimated.
44. J. P. Ferraris and G. Saito, *J. Chem. Soc. Chem. Commun.*, 992 (1978).
45. G. Saito and J. P. Ferraris, *J. Chem. Soc. Chem. Commun.*, 1027 (1979).